

GAZİ

JOURNAL OF ENGINEERING SCIENCES

Vibration Behaviors of Antisymmetric Fiber Metal Laminated Composite Plates

Sinan Maraş^a, Mustafa Yaman^b

Submitted: 18.12.2022 Revised: 21.06.2023 Accepted: 19.07.2023 doi:10.30855/gmbd.0705069

ABSTRACT

Keywords: Differential quadrature methods, fiber metal laminated composite, vibration analysis

^{a*} Ondokuz Mayıs University,
Engineering Faculty,
Dept. of Mechanical Engineering
55139 - Samsun, Türkiye
Orcid: 0000-0002-2651-374X
e mail: sinan.maras@omu.edu.tr

^b Atatürk University,
Engineering Faculty,
Dept. of Mechanical Engineering
25240 - Erzurum, Türkiye
Orcid: 0000-0002-6929-8058

*Corresponding author:
sinan.maras@omu.edu.tr

In this study, free vibration analysis of Fiber Metal Laminated (FML) composite was performed numerically. The FMLs are hybrid structures composed of fiber-reinforced polymer composites such as carbon/epoxy (CARALL), glass/epoxy (GLARE), or aramid/epoxy (ARALL) with aluminum sheets. The vibration parameters of the FML composite structures modeled by differential quadrature (DQ) methods have been determined. The natural frequencies obtained to prove the accuracy of the model are compared with the results obtained by experimental method. The effects of the change in the orientation angles of the antisymmetric carbon and glass fibers on the in-plane vibration properties of the FML plates under various boundary conditions were numerically investigated. It was concluded that the first natural frequency value of CARALL composite is 297.62 Hz, while the GLARE composite has a value of 236.59 Hz for the same boundary condition and configuration cases. Furthermore, it has been obtained that the natural frequency value of the hybrid layer sequence Al/C/G/C/Al is 278.49 Hz, and it is higher than the natural frequency value of 254.46 Hz for the sequence Al/G/C/G/Al. Another significant outcome of the research is that the highest natural frequencies were obtained in the CCCC boundary condition in all FMLs.

Antisimetrik Fiber Metal Laminat Plakaların Titreşim Davranışları

ÖZ

Bu çalışmada, Fiber Metal Laminat (FML) kompozit malzemenin serbest titreşim analizi sayısal olarak gerçekleştirilmiştir. FML'ler, karbon/epoksi (CARALL), cam/epoksi (GLARE) veya aramid/epoksi (ARALL) gibi fiber takviyeli polimer kompozitlerden oluşan ve alüminyum levhalarla desteklenen hibrit yapılar olarak tanımlanmaktadır. Diferansiyel kuadratür (DQ) yöntemiyle modellenen FML kompozit yapıların titreşim parametreleri belirlenmiştir. Modelin doğruluğunu kanıtlamak için elde edilen doğal frekanslar deneysel yöntemle elde edilen sonuçlarla karşılaştırılmıştır. Antisimetrik karbon ve cam fiberlerinin yönlenme açılarının FML levhalarının düzlem içi titreşim özellikleri üzerindeki etkisi çeşitli sınır koşulları altında sayısal olarak incelenmiştir. Aynı sınır koşulu ve konfigürasyon durumları için CARALL kompozitin birinci doğal frekans değeri 297.62 Hz olarak bulunmuştur, GLARE kompozitin ise doğal frekans değeri 236.59 Hz olarak hesaplanmıştır. Ayrıca, Al/C/G/C/Al gibi hibrit tabaka dizilimine sahip FML'nin doğal frekans değeri 278.49 Hz olarak elde edilmiştir ve bu değer, Al/G/C/G/Al dizilimi için elde edilen 254.46 Hz doğal frekans değerinden daha yüksektir. Araştırmanın bir diğer önemli sonucu, tüm FML'lerde en yüksek doğal frekanslar CCCC sınır koşulunda görülmüştür.

Anahtar Kelimeler:

Diferansiyel kareleme yöntemleri, fiber metal laminat kompozit, titreşim analizi

1. Introduction

Fiber Metal Laminates (FML) are commonly utilized especially in aircraft, aerospace and automobile industries due to their superior properties such as fatigue resistance, fatigue strength, corrosion resistance, fracture toughness and density compared to conventional materials. Since these composites are in demand in various industries, it is necessary to determine their dynamic and mechanical properties. The studies on free vibration analysis of FML composites are very limited in the literature. In these studies, the equations of motion of FML beam, plate and shell elements are generally derived using first-order (FSDT) or higher-order (HSDT) shear deformation theory. The equations have been solved by various numerical methods such as Galerkin, Rayleigh-Ritz, Finite Element method, and experimental studies have been carried out and the results have been evaluated. The effects of layer thickness, fiber orientation, boundary conditions and plate aspect ratio on vibration characteristics were investigated [1-10].

Apart from linear analyses, nonlinear vibration behaviors of these structures were also investigated. The nonlinear equations of motion of the FML plates can be obtained using the FSDT. These equations obtained to determine the nonlinear frequencies of the system can be solved using a numerical method for instance Galerkin, multiple time scale methods [11, 12].

The use of the DQ method, which is one of the numerical methods that enables to achieve results with acceptable sensitivity by using fewer elements and therefore less nodes, in the vibration behaviors of the composite beam, plate and shell elements has been quite high in recent years. From the literature survey, it is found that there are only few studies on the free vibration analysis of the FML beams and plates using DQ methods. Among these studies, Maraş and Yaman [10] used DQ methods to analyze the vibration behaviors of FML composite plates. In other studies, especially circular plate and Timoshenko beam structures have been investigated analytically and numerically [13-15].

As a result of the literature review, it has been determined that the vibration behavior of FMLs with the DQ method is not much in the published literature. It was concluded that anti-symmetric laminates were not examined in these studies. In terms of contributing to the literature in this study, the effects of anti-symmetric laminates and boundary conditions on the free vibration analysis of the FML composites were examined numerically using the DQ methods.

2. Procedure For DQ Method

The DQ method, which is one of the numerical method, gives results with acceptable precision by using less number of nodes, was introduced by Bellman and it was stated that fast and susceptible solutions of partial differential equations can be obtained in initial and boundary value problems [16]. To calculate the partial derivative of a given discrete point of a function with respect to a given space variable using the DQ method, it is necessary to find the weighted linear sum of the function values at all discrete points of that variable region [17].

For two-dimensional problems, the number of nodes in the x-direction and in the y-direction can be represented by the symbols N_x and N_y , respectively. For the discrete points (x_i, y_j) of the $u(x,y)$ function, the derivative expression of the r th order with respect to x , the derivative expression of the s th order with respect to y and the derivative expressions of the $(r+s)$ th order with respect to x and y are as follows, respectively;

$$\left. \frac{\partial^r u}{\partial x^r} \right|_{x=x_i} = \sum_{k=1}^{N_x} A_{ik}^{(r)} u(x_k, y_j) \quad r = 1, 2, \dots, N_x - 1 \quad (1)$$

$$\left. \frac{\partial^s u}{\partial y^s} \right|_{y=y_j} = \sum_{k=1}^{N_y} B_{jk}^{(s)} u(x_i, y_k) \quad s = 1, 2, \dots, N_y - 1 \quad (2)$$

$$\left. \frac{\partial^{(r+s)} u}{\partial x^r \partial y^s} \right|_{x_i y_j} = \frac{\partial^r}{\partial x^r} \left(\frac{\partial^s u}{\partial y^s} \right)_{x_i y_j} = \sum_{k=1}^{N_x} A_{ik}^{(r)} \sum_{m=1}^{N_y} B_{jm}^{(s)} u(x_k, y_m) \quad (3)$$

$i=1, 2, \dots, N_x$ ve $j=1, 2, \dots, N_y$

The expressions $A_{ij}^{(r)}$ and $B_{ij}^{(s)}$ are the weighting coefficients of the derivative expressions for the r 'th and s 'th

order x_i and y_j discrete points of the $u(x,y)$ function [18]. The weighting coefficients are obtained with the following expressions.

$$A_{ij}^{(r)} = r \left[A_{ii}^{(r-1)} A_{ij}^{(1)} - \frac{A_{ij}^{(r-1)}}{x_i - x_j} \right]; \quad i,j=1,2,\dots,N_x, \quad r=2,3,\dots,N_x-1 \quad (4)$$

$$B_{ij}^{(s)} = s \left[B_{ii}^{(s-1)} B_{ij}^{(1)} - \frac{A_{ij}^{(s-1)}}{y_i - y_j} \right]; \quad i,j=1,2,\dots,N_y, \quad s=2,3,\dots,N_y-1 \quad (5)$$

$$A_{ii}^{(r)} = - \sum_{j=1, j \neq i}^{N_x} A_{ij}^{(r)}; \quad i=1,2,\dots,N_x, \quad r=1,2,\dots,N_x-1 \quad (6)$$

$$B_{ii}^{(s)} = - \sum_{j=1, j \neq i}^{N_y} B_{ij}^{(s)}; \quad i=1,2,\dots,N_y, \quad s=1,2,\dots,N_y-1 \quad (7)$$

The relations giving the nodal point selection in x and y coordinates are as follows;

$$X_i = \frac{i-1}{N_x-1}; \quad i=1,2,\dots,N_x \quad (8)$$

$$Y_j = \frac{j-1}{N_y-1}; \quad i=1,2,\dots,N_y \quad (9)$$

In this study, the equation expressing the bending vibration of a symmetric thin-layer composite plate according to the classical plate theory is discussed. For more details on the mathematical properties of the governing equation, including its derivation and scientific applications, the interested reader may refer to [19, 20].

The DQ analogs of the vibration expression equation for inner nodes are defined as:

$$\begin{aligned} D_{11} \sum_{k=1}^{n+2} a_{ik}^{(4)} \bar{w}_{kl} + 4D_{16} \sum_{j=1}^{n+2} \sum_{k=1}^{n+2} a_{ij}^{(3)} b_{lk}^{(1)} \bar{w}_{jk} + 2(D_{12} + 2D_{66}) \sum_{j=1}^{n+2} \sum_{k=1}^{n+2} a_{ij}^{(2)} b_{lk}^{(2)} \bar{w}_{jk} \\ + 4D_{26} \sum_{j=1}^{n+2} \sum_{k=1}^{n+2} a_{ij}^{(1)} b_{lk}^{(3)} \bar{w}_{jk} + D_{22} \sum_{k=1}^{n+2} b_{lk}^{(4)} \bar{w}_{lk} = \rho h \omega^2 w_{il} \end{aligned} \quad (10)$$

$(i = 2,3, \dots, n_y - 1; l = 2,3, \dots, n_x - 1)$

where, the expressions $a_{ij}^{(1)}$, $a_{ij}^{(2)}$, $a_{ij}^{(3)}$, $a_{ij}^{(4)}$ show the weighting coefficients according to x from the first order to the fourth order, respectively. Similarly, the weighting coefficients in the y direction from the first order to the fourth order are $b_{ij}^{(1)}$, $b_{ij}^{(2)}$, $b_{ij}^{(3)}$ and $b_{ij}^{(4)}$, respectively. Also, n_x and n_y represent the total number of nodes in the x and y direction, respectively.

The DQ notations of boundary condition can be written similarly. The bending moment equations are exercised to the following partial differential derivatives: $(\partial w / \partial x)_{x=0}$ and $(\partial w / \partial x)_{x=c}$

$$\begin{aligned} D_{11} \sum_{k=1}^{n+2} a_{ik}^{(2)} \bar{w}_{kl} + D_{12} \sum_{k=1}^{n+2} b_{lk}^{(2)} \bar{w}_{lk} + 2D_{16} \sum_{j=1}^{n+2} \sum_{k=1}^{n+2} a_{ij}^{(1)} b_{lk}^{(1)} \bar{w}_{jk} = (M_x)_{il} \end{aligned} \quad (11)$$

$(i = 1,2, \dots, n_y; l = 1, n_x)$

The shear force equations are placed where the displacement expression (w) is located. The DQ equations of the boundary condition expressions are as follows:

$$\begin{aligned} D_{11} \sum_{k=1}^{n+2} a_{ik}^{(3)} \bar{w}_{kl} + 4D_{16} \sum_{j=1}^{n+2} \sum_{k=1}^{n+2} a_{ij}^{(2)} b_{lk}^{(1)} \bar{w}_{jk} + (D_{12} + 4D_{66}) \sum_{j=1}^{n+2} \sum_{k=1}^{n+2} a_{ij}^{(1)} b_{lk}^{(2)} \bar{w}_{jk} \\ + 2D_{26} \sum_{k=1}^{n+2} b_{lk}^{(3)} \bar{w}_{lk} = (V_x)_{il} \quad (i = 2,3, \dots, n_y - 1; l = 1, n_x) \end{aligned} \quad (12)$$

The equation (12) does not include the four corner points $(w_{il} (i = 1, n_y; l = 1, n_x))$.

Similarly, the DQ equations for the $(\partial w/\partial y)_{y=0}$ and $(\partial w/\partial y)_{y=d}$ cases are:

$$D_{12} \sum_{k=1}^{n+2} a_{ik}^{(2)} \bar{w}_{kl} + D_{22} \sum_{k=1}^{n+2} b_{lk}^{(2)} \bar{w}_{ik} + 2D_{26} \sum_{j=1}^{n+2} \sum_{k=1}^{n+2} a_{ij}^{(1)} b_{lk}^{(1)} \bar{w}_{jk} = (M_y)_{il} \quad (13)$$

$$(i = 1, n_y; l = 1, 2, \dots, n_x)$$

The DQ analog of shear force expression for the y coordinate can be given as follows, the equation does not include the four corner points $(w_{il} (i = 1, n_y; l = 1, n_x))$.

$$D_{22} \sum_{k=1}^{n+2} b_{lk}^{(3)} \bar{w}_{ik} + 4D_{26} \sum_{j=1}^{n+2} \sum_{k=1}^{n+2} a_{ij}^{(1)} b_{lk}^{(2)} \bar{w}_{jk} + (D_{12} + 4D_{66}) \sum_{j=1}^{n+2} \sum_{k=1}^{n+2} a_{ij}^{(2)} b_{lk}^{(1)} \bar{w}_{jk} + 2D_{16} \sum_{k=1}^{n+2} a_{ik}^{(3)} \bar{w}_{kl} = (V_y)_{il} \quad (14)$$

$$(i = 1, n_y; l = 2, 3, \dots, n_x - 1)$$

Finally, the following DQ equations are applied at the four vertices $(w_{il} (i = 1, n_y; l = 1, n_x))$:

$$2D_{16} \sum_{k=1}^{n+2} a_{ik}^{(2)} \bar{w}_{kl} + 2D_{26} \sum_{k=1}^{n+2} b_{lk}^{(2)} \bar{w}_{ik} + 4D_{66} \sum_{j=1}^{n+2} \sum_{k=1}^{n+2} a_{ij}^{(1)} b_{lk}^{(1)} \bar{w}_{jk} = R_{il} \quad (15)$$

$$(i = 1, n_y; l = 1, n_x)$$

All equations between equation (10) and equation (15) can be written in matrix form after performing the necessary mathematical operations.

$$\begin{bmatrix} K_{ee} & K_{ei} \\ K_{ie} & K_{ii} \end{bmatrix} \begin{Bmatrix} \{\Delta_e\} \\ \{w_i\} \end{Bmatrix} = \begin{Bmatrix} \{0\} \\ \lambda[I]\{w_i\} \end{Bmatrix} \quad (16)$$

The DQ analogs of the differential equation at the boundary points and all inner points are denoted by the symbols e and i, respectively. Also, the symbols $\{\Delta_e\}$, $\{w_i\}$ and $\lambda = \rho h \omega^2$ represent the displacement vector at the boundary points, the displacement vector at the inner points, and the eigenvalue expression, respectively.

After eliminating the $\{\Delta_e\}$ vector, which represents non-zero displacements, Eq. (16) can be rewritten as:

$$[K_{ii} - K_{ib} K_{bb}^{-1} K_{bi}] \{w_i\} = \lambda [I] \{w_i\} \quad (17)$$

The Equation (17) can be written in a simpler way and can be expressed as follows.

$$[\bar{K}] \{w_i\} = \lambda [I] \{w_i\} \quad (18)$$

The Equation (18) is a standard eigenvalue matrix equation and can be solved with a standard eigenvalue solver. The vector $\{w_i\}$ denoting the mode shapes can be obtained in a similar way.

3. Experimental Method

The numerical results were analogized with the experimental results to prove the accuracy and applicability of the proposed model. For this purpose, FML composite plates were produced by hot pressing method (Fig. 1). The material placed in the hot press machine was subjected to curing by heating for 2 hours at 140 °C and 20 kN force (under 5 bar pressure).



Fig. 1. FML composite plates manufactured: a) CARALL b) GLARE

The mechanical properties of the produced FML composite materials (Table 1) were obtained by applying tensile test according to ASTM D3039 standard in Shimadzu tensile machine. Then, the vibration and damping characteristics of the FML composite plates were determined using the PULSE measurement system (computer-indexed system) consisting of many measurement channels (Fig. 2).

Table 1. The mechanical properties of the materials used manufacturing the FML plates

Material	E_1 (GPa)	E_2 (GPa)	G_{12} (GPa)	ν_{12}	ρ (kg/m^3)
Carbon/epoxy	29.33	29.33	2.72	0.041	1371.4
Glass/epoxy	14.01	14.01	1.06	0.145	1627.6
Al 1050	34.00	34.00	12.78	0.330	2599.2

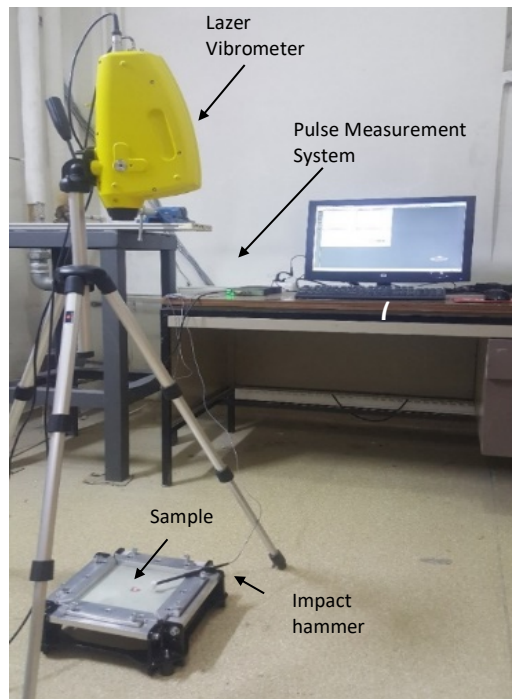


Fig. 2. Experimental Set-up

4. Experimental Validation Of The Numerical Model

The accuracy and applicability of the proposed model were shown by comparing the numerical results and the experimental results with each other. The width and length values of the FML composite plate considered in the experimental and numerical analyzes are $c=d= 0.18$ mm. The thickness of each glass prepreg, carbon

prepreg and aluminum materials are 0.18 mm, 0.25 mm and 0.3 mm, respectively. CFFC (two edges clamped and others free), CFCC (one edge free and the others clamped), and CCCC (all edges clamped) boundary conditions are discussed. It can be seen from Table 2, that there is a great agreement and accuracy between the experimental results and numerical results calculated by DQ methods.

Table 2. Comparing of the natural frequencies of the FML plates

Boundary Cond.	Layer sequence *	ω (Hz)			
		Solution Methods			
		DQ	ANSYS	Experimental	Error percentage# (%)
CCCC	A1	403.8	399.3	412.1	2.1
	A2	357.0	353.6	362.5	1.5
CFCC	A1	264.9	262.2	275.1	3.8
	A2	233.1	230.9	237.5	1.9
CFFC	A1	89.2	76.7	80.1	10.2
	A2	78.8	67.8	75.2	4.6

* $A_1 = (Al-G_{45^\circ/45^\circ}-G_{30^\circ/60^\circ}-G_{45^\circ/45^\circ}-G_{30^\circ/60^\circ})_s$; $A_2 = (G_{30^\circ/60^\circ}-Al-G_{30^\circ/60^\circ}-G_{45^\circ/45^\circ}-G_{30^\circ/60^\circ})_s$; Al=Aluminium ; G_θ : Glass prepreg; θ :Fiber orientation angle; # Error percentage# (%): Percentage difference value of the experimental result and the DQ method result.

5. Numerical Analysis

In this study, the effects of changes in the number of layers, fiber orientation angles and material properties on the natural frequencies of the FML composites in various anti-symmetric configurations as shown in Table 3, Table 4 and Table 5 were investigated.

Table 3. The configurations of GLARE

GLARE				
Group	Number of layers	of	Lay-up sequence	Orientation angle
G1	3		Al /G/ Al	
G2	5		Al /G/G/G/ Al	0°/90°
G3	7		Al /G/G/G/G/G/ Al	
G4	3		Al /G/ Al	
G5	5		Al /G/G/G/ Al	30°/60°
G6	7		Al /G/G/G/G/G/ Al	
G7	3		Al /G/ Al	
G8	5		Al /G/G/G/ Al	45°/-45°
G9	7		Al /G/G/G/G/G/ Al	

Table 4. The configurations of CARALL

CARALL				
Group	Number of layers	of	Lay-up sequence	Orientation angle
C1	3		Al /C/ Al	
C2	5		Al /C/C/C/ Al	0°/90°
C3	7		Al /C/C/C/C/C/ Al	
C4	3		Al /C/ Al	
C5	5		Al /C/C/C/ Al	30°/60°
C6	7		Al /C/C/C/C/C/ Al	
C7	3		Al /C/ Al	
C8	5		Al /C/C/C/ Al	45°/-45°
C9	7		Al /C/C/C/C/C/ Al	

Table 5. The configurations of HYBRID FMLs

HYBRID FMLs			
Group	Lay-up sequence	Orientation angle	Number of layers
H1	Al /C/G/C/ Al	0°/90°	5
H2	Al /G/C/G/ Al		
H3	Al /C/G/C/ Al	30°/60°	
H4	Al /G/C/G/ Al		
H5	Al /C/G/C/ Al	45°/-45°	
H6	Al /G/C/G/ Al		

6. Results And Discussions

The effects of the change in the fiber orientation angles of the GLARE FMLs under the CCCC boundary condition on the free vibrations of the structure is shown in Fig. 3. It is seen that there is no significant change in the natural frequencies of the plate depending on the change in fiber orientation angles. This is because glass fiber prepreps have a plain weave. The mechanical properties of these prepreps in the transverse and longitudinal directions are very similar to each other. Thus, the stiffness of the composite structure and hence its natural frequencies are not considerably impressed by the change in fiber orientation angles. Also, as the number of glass fiber layers in the structure increased, the natural frequencies also increased. Similar trend is noticed in the study of comparative dynamic analysis of carbon, aramid and glass fiber reinforced interply and intraply hybrid composites by Aydın, et al. [21]. The reason for this is that by adding a glass fiber/epoxy layer to the structure, the rigidity of the plate increases with the increase in the number of layers of the structure. On the other hand, the mass amount of the composite structure also increases. As a result, the increase in the frequencies seen in the graphs reveals that the improvement in the rigidity of the structure is more dominant.

The effects of the change in the fiber orientation angles of the GLARE FMLs under the CFCC boundary condition on the free vibrations of the structure is shown in Fig. 4. Similar to Fig. 3, it is seen that the change of fiber angles does not cause a significant change on natural frequencies for the structure under the CFCC boundary condition.

The factors affecting the natural frequency of the FML plate are stiffness, density, and mass moment of inertia. Apart from these, it is observed that natural frequencies decrease significantly as the number of free edges of the composite structure increases (Fig. 5). The natural frequencies of FMLs under free edge boundary conditions are considerably lower than those of fully clamped FMLs due to the change in the restraint effect at the edges. Thus, unlike other boundary conditions, a composite structure with a clamped boundary condition increases its stiffness and thus its natural frequencies. When the relevant studies in the literature supporting this inference are examined, E. V. Prasad and S. K. Sahu concluded that the boundary conditions is more sensitive to the natural frequencies of plates [8].

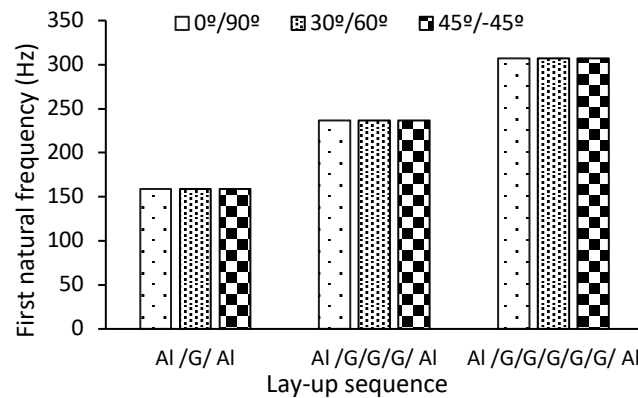


Fig. 3. GLARE FMLs under CCCC boundary conditions

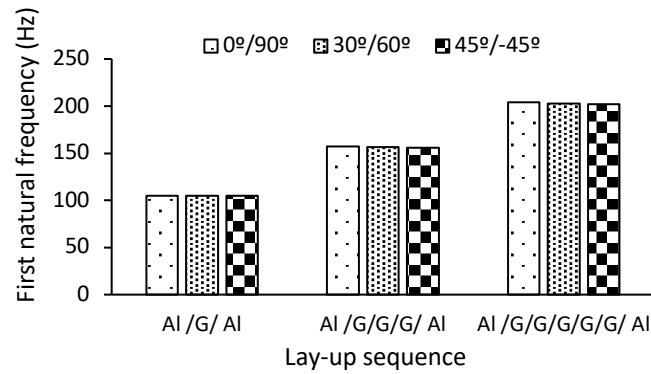


Fig. 4. GLARE FMLs under CFCC boundary conditions

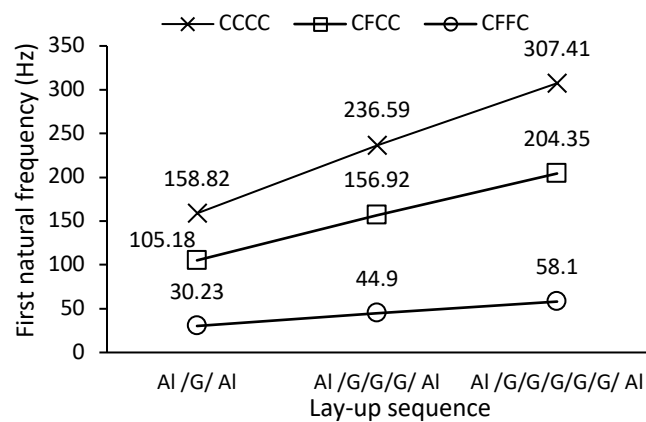


Fig. 5. GLARE FMLs under different boundary conditions

The effects of variation in fiber orientation angles of the carbon prepregs in the interlayers on the free vibrations of the structure for CARALL FMLs composites under the CCCC boundary condition are presented in Fig. 6.

The lay-up was designed as given configuration in Table 4 where the orientation angles $\theta = 0^\circ/90^\circ, 30^\circ/60^\circ, 45^\circ/45^\circ$.

The Fig. 6 is examined, it can be said that there is no significant change in the natural frequencies of the plate even though the change in fiber orientation angles. The reason can be clarified as follows: carbon fiber prepregs are plain woven, so their mechanical properties are close to each other in the longitudinal and transverse directions. Therefore, there is no appreciable effect on the stiffness of the composite structure despite the change in fiber orientation angles. It was also observed that the highest natural frequencies were obtained as the number of carbon fiber/epoxy layers in the structure increased. Similar trend is noticed in the study Free vibration analysis of fiber metal laminated straight beam by Maraş, et al. [22].

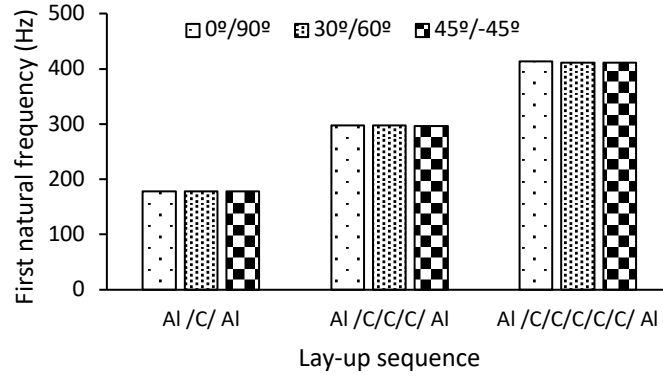


Fig. 6. CARALL FMLs under CCCC boundary conditions

The effects of various boundary conditions on the vibration behavior of the CARALL structure are examined in Fig. 7. The results show that the highest natural frequency values for the same sequence conditions of the layers have obtained at the CCCC boundary condition where the stiffness is higher.

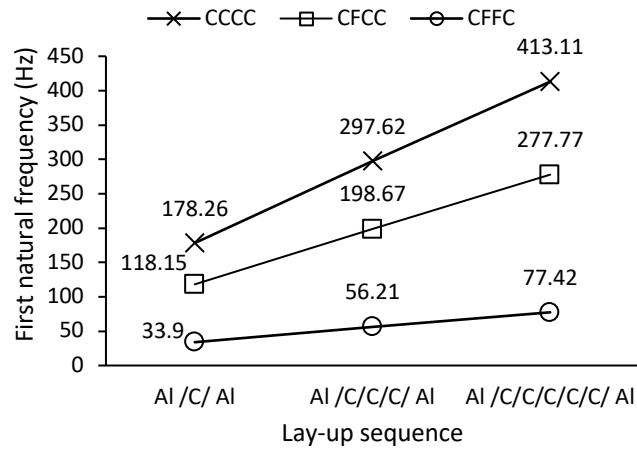


Fig. 7. CARALL FMLs under different boundary conditions

Fig. 8 shows the distribution plot of the natural frequencies obtained versus the change in fiber orientation angle for the hybrid FML composites given in Table 5. As a result of the change in fiber orientation angle, it is seen that there is no notable change in natural frequencies. Besides, the natural frequencies change with the change in fiber type.

The effect of placing the variable fiber type in the inner layers on the vibration properties was investigated in Fig. 9. It is seen that the natural frequency values of the structure increase as the number of carbon fiber epoxy layers in the structure increases by placing carbon fiber/epoxy layer instead of a glass fiber/epoxy layer. Supporting this result, in the study by Utomo, et al. [23], examining the influence of the number and position of the carbon fiber lamina on the natural frequency and damping ratio of the carbon-glass hybrid composite, it is determined that there is a significant decrease in natural frequency with the increase of the glass fiber laminates in the structures. The reason is that taking into consideration the material properties given in Table 1 as the number of carbon/epoxy layers increases, the density of the structure decrease.

Moreover, it is obtained that the natural frequency value of the Al /C/G/C/ Al sequence is higher than the natural frequency value of the Al /G/C/G/ Al sequence from the hybrid layer sequences (Fig. 9). This is because the lateral stiffness of the carbon/epoxy layer is higher than that of the glass/epoxy layers. Another reason is that the mass moment of inertia of the structure has a lower value if the glass fiber/epoxy layer is placed towards the center of the structure. When the relevant studies in the literature supporting this inference are examined, Muddappa, et al. [24] concluded that different hybrid configurations play an important role in the vibration behavior of the FML plate. They determined that the natural frequency of the plate is higher if

the outermost layers have a carbon fiber/epoxy layer instead of glass fiber/epoxy.

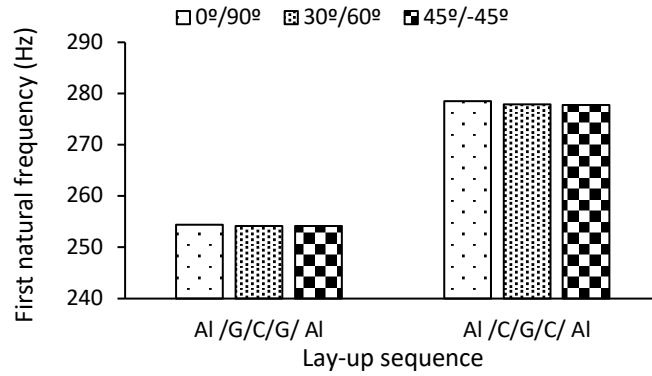


Fig. 8. Hybrid FMLs under CCCC boundary conditions

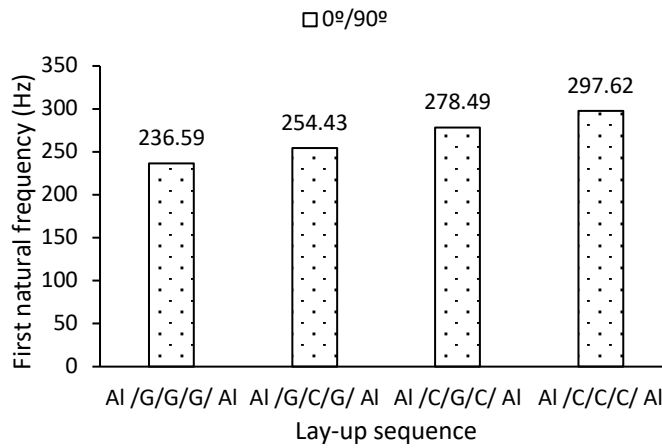


Fig. 9. Effects of fiber type changes on natural frequencies in 5-layer FML composites under CCCC boundary conditions

The natural frequencies of hybrid FML composites with 0°/90° fiber orientation angles were compared by changing the boundary conditions (CCCC, CFCC, CFFC) (Fig. 10).

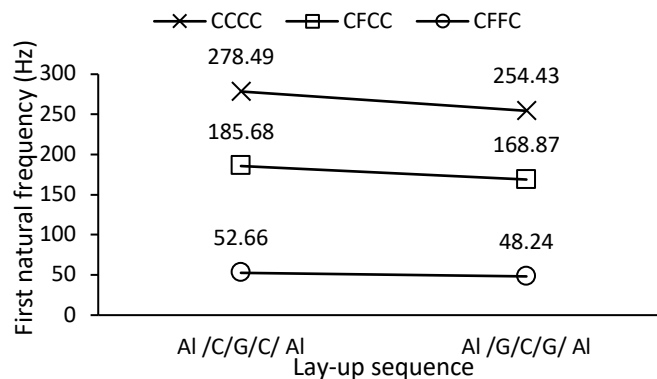


Fig. 10. Hybrid FMLs under different boundary conditions

Since the stiffness of the structure is higher in the CCCC boundary condition than in other boundary conditions, the natural frequency value of the structure is the highest in this boundary condition. Similar trend is noticed in the study Free vibration analysis of fiber metal laminated plates by Prasad and Sahu [25].

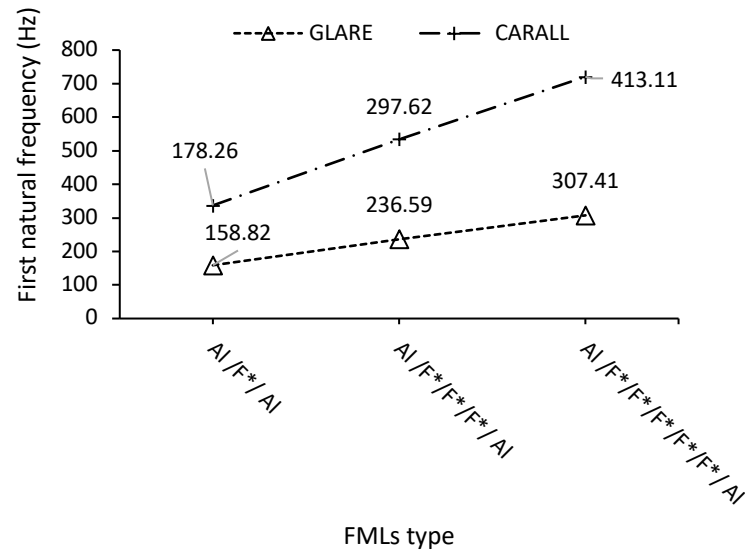


Fig. 11. Comparison of the first natural frequency of GLARE and CARALL composite plates

The comparison of natural frequencies of GLARE and CARALL composites under CCCC boundary condition and having the same configuration is given in Fig. 11. Here, the F* symbol denotes the fiber type in the form of glass fiber or carbon fiber. If the Fig. 11 is examined, it is seen that the natural frequencies of GLARE composites are lower than those of CARALL composites. This is based on glass prepregs with a lower elasticity modulus and higher density than carbon prepregs. When using a glass prepreg instead of a carbon prepreg, the density of the structure and the mass moment of inertia increase, resulting in a decrease in the natural frequency of the plates. In the study conducted by Utomo, et al. [23], which supports this result, it was determined that adding more carbon layers to the carbon-glass hybrid composite results in an increase in the natural frequency of the composite material.

6. Conclusion

In this study, free vibration behavior of GLARE, CARALL and Hybrid FML composites with antisymmetric lay-up was investigated by DQ method. From the examined configurations, the following determinations can be made.

- It was observed that there was no significant change in the natural frequencies of the plates, although the fiber orientation angles were changed in all FMLs examined.
- The highest natural frequencies were obtained in the CCCC boundary condition in all FMLs. It was cleared that as the number of free edges in the composite structure increases, the natural frequencies decrease significantly.
- It was also determined that the highest natural frequencies were obtained as the number of carbon fiber epoxy layers in the structure increased by placing a carbon fiber/epoxy layer instead of a glass fiber/epoxy layer.
- It was concluded that the first natural frequency values of CARALL composites were found to be higher than GLARE composites for the same boundary condition and configuration cases.

Conflict of Interest Statement

The authors declare that there is no conflict of interest.

References

- [1] R. Kolar, "Dynamic characteristics of layered metal-fiber composites including transverse shear deformation," *Smart Materials II*, 2002, vol. 4934: SPIE, pp. 270-278. doi:<https://doi.org/10.1117/12.469170>

- [2] H. Ravishankar, R. Rengarajan, K. Devarajan and B. Kaimal, "Free vibration behaviour of fiber metal laminates, hybrid composites, and functionally graded beams using finite element analysis," *International Journal of Acoustics and Vibration*, vol. 21, no. 4, pp. 418-428, 2016. doi: <https://doi.org/10.20855/ijav.2016.21.4436>
- [3] C. Tao, Y. Fu and T. Dai, "Dynamic analysis for cracked fiber-metal laminated beams carrying moving loads and its application for wavelet based crack detection," *Composite Structures*, vol. 159, pp. 463-470, 2017. doi: <https://doi.org/10.1016/j.compstruct.2016.09.087>
- [4] B. Han, W. Hui, Q. C. Zhang, Z. Y. Zhao, F. Jin, Q. Zhang, T. J. Lu and B. H. Lu, "A refined quasi-3D zigzag beam theory for free vibration and stability analysis of multilayered composite beams subjected to thermomechanical loading," *Composite Structures*, vol. 204, pp. 620-633, 2018. doi: <https://doi.org/10.1016/j.compstruct.2018.08.005>
- [5] B. HARRAS, R. Benamar and R. White, "Experimental and theoretical investigation of the linear and non-linear dynamic behaviour of a glare 3 hybrid composite panel," *Journal of Sound and Vibration*, vol. 252, no. 2, pp. 281-315, 2002. doi: <https://doi.org/10.1006/jsvi.2001.3962>
- [6] A. Secgin, C. Atas and A. S. Sarigül, "The effects of composite plate design parameters on linear vibrations by discrete singular convolution method," *Journal of Composite Materials*, vol. 43, no. 24, pp. 2963-2986, 2009. doi: <https://doi.org/10.1177/0021998309345>
- [7] F. A. Ghasemi, R. Paknejad and K. M. Fard, "Effects of geometrical and material parameters on free vibration analysis of fiber metal laminated plates," *Mechanics & Industry*, vol. 14, no. 4, pp. 229-238, 2013. doi: <https://doi.org/10.1051/meca/2013062>
- [8] E. Prasad and S. Sahu, "Vibration analysis of woven fiber metal laminated plates—experimental and numerical studies," *International Journal of Structural Stability And Dynamics*, vol. 18, no. 11, p. 1850144, 2018. doi: <https://doi.org/10.1142/S0219455418501444>
- [9] A. R. Ghasemi and M. Mohandes, "Free vibration analysis of micro and nano fiber-metal laminates circular cylindrical shells based on modified couple stress theory," *Mechanics of Advanced Materials and Structures*, vol. 27, no. 1, pp. 43-54, 2020. doi: <https://doi.org/10.1080/15376494.2018.1472337>
- [10] S. Maraş and M. Yaman, "Free vibration analysis of fiber-metal laminated composite plates using differential, generalized and harmonic quadrature methods: experimental and numerical studies," *Engineering Computations*, vol. 39, no. 6, pp. 2326-2349, 2022. doi: <https://doi.org/10.1108/EC-08-2021-0490>
- [11] A. Shooshtari and S. Razavi, "Nonlinear free and forced vibrations of anti-symmetric angle-ply hybrid laminated rectangular plates," *Journal of Composite Materials*, vol. 48, no. 9, pp. 1091-1111, 2014. doi: <https://doi.org/10.1177/0021998313482156>
- [12] C. Tao, Y.-M. Fu and H.-L. Dai, "Nonlinear dynamic analysis of fiber metal laminated beams subjected to moving loads in thermal environment," *Composite Structures*, vol. 140, pp. 410-416, 2016. doi: <https://doi.org/10.1016/j.compstruct.2015.12.011>
- [13] Y. Fu, Y. Chen and J. Zhong, "Analysis of nonlinear dynamic response for delaminated fiber-metal laminated beam under unsteady temperature field," *Journal of Sound and Vibration*, vol. 333, no. 22, pp. 5803-5816, 2014. doi: <https://doi.org/10.1016/j.jsv.2014.06.015>
- [14] X. Shao, Y. Fu and Y. Chen, "Nonlinear dynamic response and active control of fiber metal laminated plates with piezoelectric actuators and sensors in unsteady temperature field," *Smart Materials and Structures*, vol. 24, no. 5, p. 055023, 2015. doi: [10.1088/0964-1726/24/5/055023](https://doi.org/10.1088/0964-1726/24/5/055023)
- [15] H. Moraveji Tabasi, J. Eskandari Jam, K. Malekzadeh Fard and M. Heydari Beni, "Buckling and free vibration analysis of fiber metal-laminated plates resting on partial elastic foundation," *Journal of Applied and Computational Mechanics*, vol. 6, no. 1, pp. 37-51, 2020. doi: [10.22055/JACM.2019.28156.1489](https://doi.org/10.22055/JACM.2019.28156.1489)
- [16] Z. A. Siddiqi, "Analysis of interacting subdomains in structural mechanics problems by the differential quadrature method," Ph.D. dissertation, The University of Oklahoma, Norman, Oklahoma, 1995.
- [17] R. Bellman and J. Casti, "Differential quadrature and long-term integration," *Journal of mathematical analysis and Applications*, vol. 34, no. 2, pp. 235-238, 1971. doi: [https://doi.org/10.1016/0022-247X\(71\)90110-7](https://doi.org/10.1016/0022-247X(71)90110-7)
- [18] C. Shu and B. E. Richards, "Application of generalized differential quadrature to solve two-dimensional incompressible Navier-Stokes equations," *International Journal for Numerical Methods in Fluids*, vol. 15, no. 7, pp. 791-798, 1992. doi: <https://doi.org/10.1002/flid.1650150704>
- [19] L. P. Kollar and G. S. Springer, *Mechanics of composite structures*. Cambridge university press, 2003.
- [20] R. F. Gibson, *Principles of composite material mechanics*. CRC press, 2016.
- [21] M. R. Aydin, V. Acar, F. Cakir, Ö. Gündoğdu and H. Akbulut, "Comparative dynamic analysis of carbon, aramid and glass fiber reinforced interply and intraply hybrid composites," *Composite Structures*, vol. 291, p. 115595, 2022. doi: <https://doi.org/10.1016/j.compstruct.2022.115595>
- [22] S. Maraş, M. Yaman, M. F. Şansveren and S. K. Reyhan, "Free vibration analysis of fiber metal laminated straight beam," *Open Chemistry*, vol. 16, no. 1, pp. 944-948, 2018. doi: <https://doi.org/10.1515/chem-2018-0101>
- [23] J. T. Utomo, D. D. Susilo and W. W. Raharja, "The influence of the number and position of the carbon fiber lamina on the natural frequency and damping ratio of the carbon-glass hybrid composite," in *International Conference on Engineering, Science and*

Nanotechnology, vol. 1788, no. 1: Solo, Indonesia:AIP Publishing, 2017. pp. 1-6.

[24] P. Y. Muddappa, T. Rajanna and G. Giridhara, "Effects of different interlaminar hybridization and localized edge loads on the vibration and buckling behavior of fiber metal composite laminates," *Composites Part C: Open Access*, vol. 4, p. 100084, 2021. doi:<https://doi.org/10.1016/j.jcomc.2020.100084>

[25] E. Prasad and S. Sahu, "Free vibration analysis of fiber metal laminated plates," in *International Conference on Theoretical, Applied, Computational and Experimental Mechanics*, Kharagpur, India: Proceedings of ICTACEM, 2017. pp. 1-10.

* *This article is an extended version of the paper presented at the International Conference on Engineering Technologies (ICENTE'22)*

This is an open access article under the CC-BY license

